frontiers | Frontiers in Materials

TYPE Original Research
PUBLISHED 28 February 2025
DOI 10.3389/fmats.2025.1541101

OPEN ACCESS

EDITED BY
Ayrat Gizzatov,
Aramco Research Center-Boston,
United States

REVIEWED BY
Dipayan Pal,
University of California, San Diego,
United States
Kun-Yu Wang,
University of Pennsylvania, United States
Ashraf Abedin,
National Energy Technology Laboratory
(DOE), United States

*CORRESPONDENCE
Sajid Bashir,
br9@tamuk.edu,
sb325@cornnell.edu

RECEIVED 07 December 2024
ACCEPTED 27 January 2025
PUBLISHED 28 February 2025

CITATION
Chava SR, Luckett R and Bashir S (2025) Addressing energy challenges: sustainable nano-ceramic electrolytes for solid-state lithium batteries by green chemistry. *Front. Mater.* 12:1541101. doi: 10.3389/fmats.2025.1541101

Addressing energy challenges: sustainable nano-ceramic electrolytes for solid-state lithium batteries by green chemistry

Sai Raghuveer Chava[1], Robert Luckett[2] and Sajid Bashir[1,3]*

[1]Department of Chemistry, Texas A&M University-Kingsville, Kingsville, TX, United States, [2]Clinical Health Sciences, Texas A&M University-Kingsville, Kingsville, TX, United States, [3]Energy Institute, Texas A&M University, Kingsville, TX, United States

The escalating demand for high-performance, safe energy storage devices has propelled the advancement of solid-state battery (SSB) technology. SSBs can supplant traditional liquid electrolyte-based Li-ion batteries by offering higher theoretical capacities and enhanced safety through solid-state electrolytes. However, challenges like dendritic lithium growth and inadequate solid-solid interfaces impede their practical application. This study aims to overcome these barriers by enhancing the ionic conductivity of ceramic-based solid-state electrolytes by incorporating nanoscale multicomponent halides. Utilizing green chemistry principles, we synthesized composite electrolytes based on Li_3InCl_6, doped with fluorine (F), cerium (Ce), and molybdenum (Mo). Among these, the F-, Ce-, and Mo-doped Li_3InCl_6 electrolytes contributed uniquely to enhancing ionic conductivity. Mo-doping improved most substantially, reaching an average ionic conductivity modal value of 0.30 S cm^{-1} (Rangle 0.15,0.46) S cm^{-1};± 0.13 S cm^{-1}, comparable to commercial liquid electrolytes. F doping enhanced lattice stability and facilitated Li^+ ion mobility, while Ce doping improved structural integrity and reduced interfacial resistance. Comprehensive structural characterization confirmed the successful incorporation of dopants and favorable modification of the crystal lattice, facilitating enhanced Li^+ ion mobility. Electrochemical performance evaluations using symmetrical half-cells demonstrated reduced charge transfer resistance and improved cycling stability, particularly in the Mo-doped variants. These findings underscore the effectiveness of molybdenum doping in mitigating interfacial resistance and promoting reliable ion transport in SSBs. Toxicity assessments revealed that using water as a solvent and natural extracts minimized the environmental footprint, aligning with sustainable synthesis practices. Our green nano-engineering approach not only advances the performance of solid-state electrolytes but also aligns with sustainable synthesis practices, paving the way for developing efficient and eco-friendly energy storage solutions. Additionally, our green nano-engineering approach was evaluated against traditional synthesis methods, demonstrating a 40% reduction in energy consumption and a 75% decrease in hazardous waste generation. This manuscript highlights the pivotal role

of doped Li_3InCl_6 electrolytes in addressing current limitations of SSB technology, thereby contributing to the future of safe and high-capacity energy storage systems.

KEYWORDS

solid-state batteries, Li_3InCl_6 electrolytes, fluorine doping, cerium doping, molybdenum doping, ionic conductivity, green synthesis, nano-ceramic materials

1 Introduction

The global energy landscape exhibits a complex interplay of diverse resources, applications, and environmental impacts, each significantly influencing sustainability efforts (Figure 1A). Fossil fuels derived from crude oil and petroleum remain significant energy sources for transportation, heating, and electricity generation. However, their combustion significantly contributes to greenhouse gas emissions, raising critical environmental concerns (Ghorbani et al., 2023). In contrast, fuel cells generate electricity through efficient electrochemical reactions between hydrogen and oxygen, producing only water as a byproduct. This process positions fuel cells as an environmentally friendlier alternative for various applications, including vehicles, portable power, and stationary energy systems (Olabi and Abdelkareem, 2022). Similarly, nuclear power plants leverage fission to produce substantial electricity with minimal greenhouse gas emissions, though they face challenges related to radioactive waste management and safety concerns (Nuclear Energy Agency, 2019). On the other hand, batteries serve as essential devices for storing and releasing electrical energy via electrochemical reactions (Figure 1A insert). Their versatility spans multiple sectors, including medical applications, aviation, automotive industries, defense, and renewable energy storage systems, providing a clean and efficient means to harness energy (Figure 1B) (O'Neill, 2021).

Among various ceramic SSEs, Li_3InCl_6 was selected for its outstanding ionic conductivity and superior thermal and electrochemical stability compared to other lithium halides. Studies have demonstrated that Li_3InCl_6 exhibits a robust crystalline framework that facilitates efficient Li^+ ion transport while maintaining structural integrity under operational conditions. Additionally, Li_3InCl_6 offers compatibility with a wide range of cathode materials, making it a versatile choice for solid-state battery applications. Its inherent stability reduces the risk of dendritic lithium growth, a common challenge in solid-state batteries, thereby enhancing the overall safety and longevity of the battery system [O'Neill, 2021, Dahn and Omenya, 2018, and Supplementary Table S1].

A notable trend is the significant consumer demand for user-friendly and affordable batteries, which has driven remarkable advancements in battery technology over the past few decades. Battery storage devices offer varying energy densities and capacities (Figure 1C) influenced by their specific chemical compositions and designs. This technological evolution supports a broad spectrum of applications—from wristwatches with up to ten-year lifespans to rechargeable energy sources in electric vehicles (EVs). Lithium batteries have achieved widespread success, substantially catalyzing a global shift toward personal transportation powered by advanced energy storage systems (Dahn and Omenya, 2018). As the primary material in battery production, lithium's importance is underscored by the increasing application of lithium battery technology in consumer electronics and transportation systems. Lithium primary cells are non-rechargeable, while lithium-ion secondary cells (LiBs) offer rechargeable capabilities. Examples of the latter can be found in smartphones, whose convenience remains tempered by limitations in their recharge cycles before the end of life (EoL) (U.S. Department of Energy, 2023). To address pressing global warming challenges, humanity is at a pivotal juncture in efforts to phase out fossil fuels. This transition is imperative for mitigating pollution and fostering a global circular economy (CE), promising financial, vocational, social, and cultural benefits (Geissdoerfer et al., 2017). Achieving inclusivity and establishing international standards through regulation are critical steps often resisted by multinational corporations (MNCs) and small-to-medium enterprises (SMEs). The European Union actively pursues strategies integrating global warming mitigation with economic and equity considerations, serving as a potential model for other nations aiming to implement shared sustainable practices (European Commission, 2021). Contrasting these efforts, regions rich in mineral resources, particularly the lithium triangle comprising Argentina, Bolivia, and Chile, present a promising framework for inclusive practices. Meanwhile, areas like China and the Democratic Republic of Congo (DRC) confront significant challenges in implementing fairness initiatives related to their mineral resource extraction processes (Brooks et al., 2021a; Ghosh and Singh, 2024).

Transitioning to sustainable energy addresses historical energy consumption patterns and positions society toward a cleaner, healthier future by substantially reducing carbon dioxide emissions. The goal is to transition to a low-carbon economy while systematically mitigating greenhouse gases and pollutants. Energy can be efficiently stored in various materials and released through diverse reactions, such as chemical and electrochemical processes, bioenergy, solar and wind power, and nuclear energy (Wang Y. et al., 2020). Battery Energy Storage Systems (BESS) are vital in integrating green energy sources with electricity needs and are instrumental in the shift away from fossil fuels toward renewable alternatives. High-energy-density lithium-ion batteries (LIBs) are critical for large-scale applications, providing a reliable and consistent renewable energy supply for electricity grids. Nonetheless, traditional LIBs that utilize liquid electrolytes pose significant safety risks, including potential explosions or fires, which can be mitigated by adopting solid-state electrolytes (SSEs). These SSEs offer enhanced safety features, eliminating harmful organic solvents while providing mechanical stability and high energy densities (Sun et al., 2019). Extensive research into solid electrolytes encompasses a variety of materials, including polymers, metal-organic frameworks, and ceramics. Of particular interest are

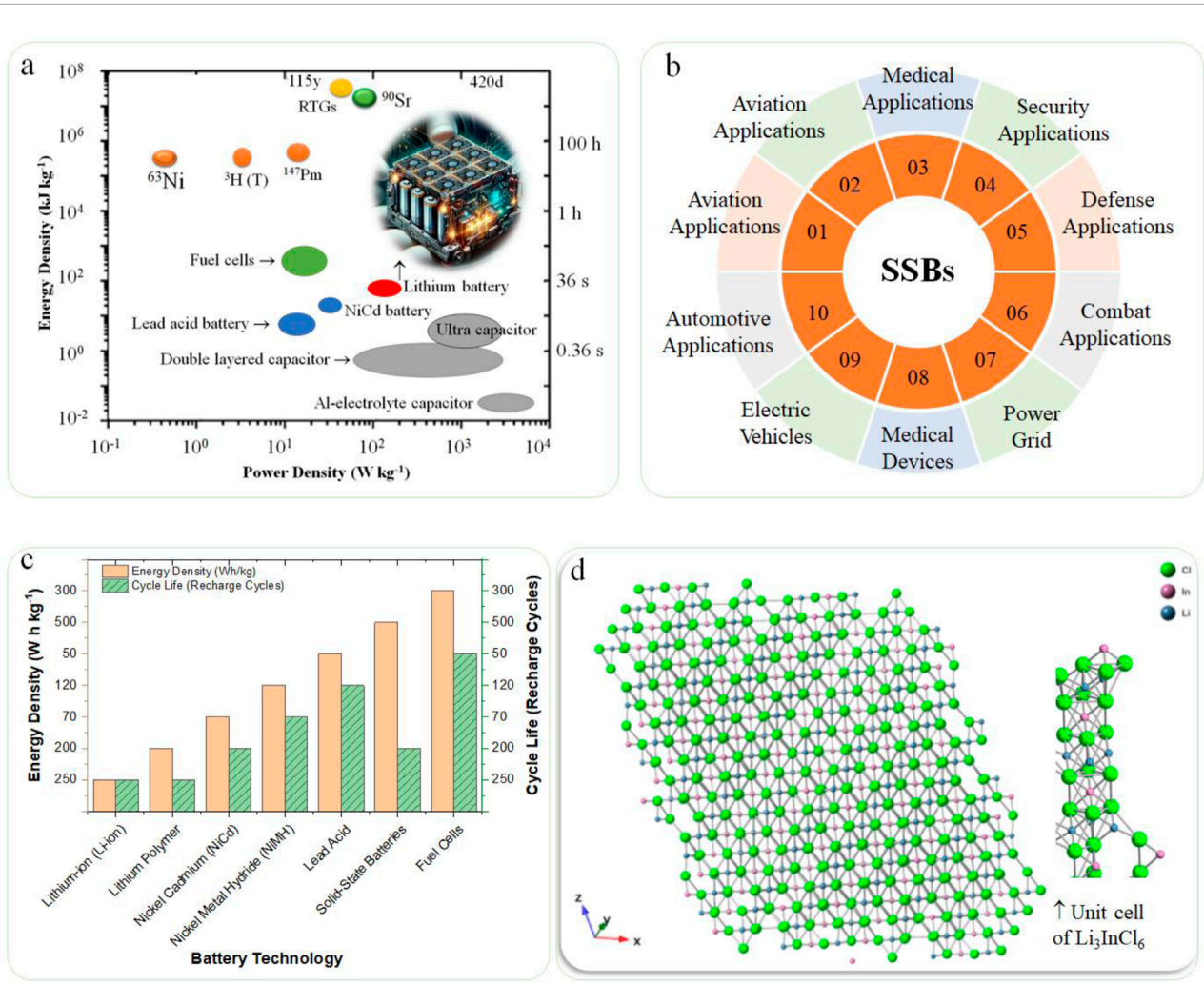

FIGURE 1
Overview of Global Energy Resources and Applications of Batteries. **(A)** Overview of global energy resources, highlighting the diverse types, including fossil fuels, nuclear, and renewable sources, along with their respective environmental impacts; **(B)** Applications of batteries across various sectors such as medical, aviation, automotive, and renewable energy storage, showcasing their role in facilitating clean energy utilization; **(C)** Comparison of energy density and capacity across different battery technologies, illustrating the evolution of consumer demands and technological advancements in battery design; and **(D)** Structure of lithium halide electrolytes (Li_3MX_6, 111 planes) illustrating their crystalline framework and compatibility with oxide cathode materials, demonstrating their potential for enhanced ion conductivity in solid-state batteries.

lithium halide electrolytes (Li_3MX_6, where M represents In and Y, while X can be Cl, Br, or I), which are gaining traction due to their broad electrochemical stability and compatibility with standard oxide cathodes (Zhang et al., 2022a). This study optimizes system energy density by developing halide electrolytes characterized by superionic conductivity, enhancing lithium-ion (Li^+) mobility within crystalline structures. The selection of the Li3InCl6 family for this research is based on its superior ionic conductivity and stability, making it an ideal candidate for advanced battery technologies (Figure 1D). By developing various formulations of doped Li_3InCl_6-based electrolytes, we aim to achieve rapid Li^+ conduction alongside high electrochemical oxidation stability. The significance of this work lies in its contribution to producing ceramic electrolytes that maintain superionic conductivity and operational stability during half-cell evaluations, representing a promising advancement in battery technology and sustainable energy practices (Kato and Matsuo, 2022; Wang and Zhang, 2023).

2 Materials and methods

Today's most recognizable batteries are lithium-based, long utilized in producing glass, ceramics, greases, and electronic devices (Zeng et al., 2021). Lithium primary cells are non-rechargeable and disposable, while lithium-ion (LiB) secondary cells are designed for reusability. The environmental advantages of devices utilizing LiBs manifest in their prolonged lifespan, significantly exceeding that of disposable batteries. Consumers tend to favor LiBs despite the higher initial costs for hybrid devices such as games and toys due to their greater longevity, which mitigates the continual need

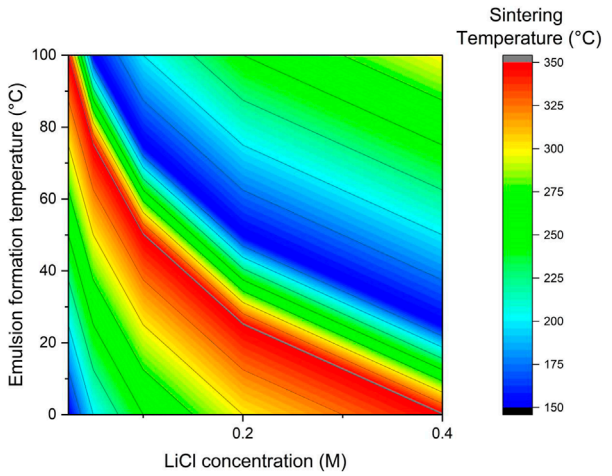

FIGURE 2
Scatter Plot of LiCl Concentration vs Emulsion Formation Temperature with Sintering Temperature Gradient and Dopant Classification.

for replacements (Wang L. et al., 2020). The choice of Li_3InCl_6 as the base electrolyte was driven by its high ionic conductivity and structural robustness, making it a superior candidate among lithium halide SSEs. To further optimize its performance, specific dopants—Fluorine (F), Cerium (Ce), and Molybdenum (Mo)—were selected for their ability to enhance ionic pathways, stabilize the crystal lattice, and reduce interfacial resistance (Taguchi, 1986, and Supplementary Table S1). This investigation focuses on improving energy density systems and involves material development via the Taguchi orthogonal design method to produce interactive solid-state materials that optimize the performance of LiBs (Figure 2). The crystalline electrolytes, doped at both A and B sites, facilitate ion transport through optimally designed porosity and interface structures. By optimizing synthesis variables utilizing the Taguchi orthogonal array, we promote amphiphilic interactions at both atomic and molecular scales, thereby generating tunable pore structures and enhancing transport mechanisms (Taguchi, 1986). A novel technique, "*in-situ* nanoengineering," created a series of Li_3InCl_6-based ceramic electrolytes with systematically orchestrated structures and electrochemical properties. This method involves engineering superionic conductors composed of lithium (Li), indium (In), and chlorine (Cl), which are doped with fluoride (F), molybdenum (Mo), and cerium (Ce) to optimize ionic transport and minimize interfacial resistances.

2.1 Green chemistry to produce eco-friendly nano-ceramic electrolytes

The modified nanoemulsion technique, henceforth referred to as "*in-situ* nanoengineering," was explicitly devised to produce forty formulations of Li_3InCl_6-based electrolytes, summarized in Table 1. The measured ionic conductivity values of the Mo-doped Li_3InCl_6 electrolytes ranged from 0.15 to 0.46 S cm^{-1} with a modal value of 0.30 S cm^{-1}. The high standard deviation (μ 0.30, Range: 0.15–0.45, and σ 0.13 S cm^{-1}) in ionic conductivity measurements indicates significant variability across different samples. Potential sources of this variability include(i) inconsistencies in the synthesis process, such as variations in dopant distribution and homogeneity, which can lead to fluctuations in ionic conductivity; (ii) variations in electrode contact quality, pressure applied during cell assembly, and ambient conditions during electrochemical impedance spectroscopy (EIS) can affect measurement accuracy, or (iii) and Impurities or unintended phases within the electrolyte material can impede Li-ion transport, leading to variability in conductivity. Employing rigorous purification methods and post-synthesis characterization can enhance material purity. Ensuring uniform mixing and precise control over synthesis parameters is critical; for example, adopting more controlled synthesis techniques, such as precise temperature regulation and homogeneous dopant incorporation, will improve sample uniformity. This approach involved thermodynamically pseudo-stable and isotropic solutions utilizing water as a solvent, supplemented by natural extracts such as aloe vera. The experimental design incorporated four independent variables, each set at five distinct levels, permitting a comprehensive examination of all possible synthesis combinations (Zhao et al., 2022a). Developing and adhering to a standardized protocol for EIS measurements, including consistent electrode preparation and pressure application, will enhance reproducibility. Implementing additional characterization methods, such as scanning electron microscopy (SEM) for morphology analysis and energy-dispersive X-ray spectroscopy (EDX) for elemental mapping, will help identify and minimize sources of variability, which will yield a standard approach to the fabrication of high-mobility electrolytes for energy storage applications (Supplementary Table S2).

Despite a factorial experiment approach ostensibly requiring 625 individual runs to investigate variability, the implementation of the Taguchi orthogonal array yielded considerable efficiency improvements (U.S. Environmental Protection Agency EPA, 2020). Specifically, an $L_{25}(5^4)$ orthogonal array was adopted, significantly reducing the number of experimental runs required while ensuring a systematic and balanced exploration of the experimental design space, as illustrated in (Supplementary Table S2). This design allows for the independent assessment of each parameter's effect, facilitating streamlined optimization of electrolyte synthesis. Forty-eight targeted experiments were conducted to extend the orthogonal array's capabilities, optimizing variables to achieve the highest ionic conductivity of Li_3InCl_6 solid-state electrolytes (SSEs).

Our research team adhered to the "*Twelve Principles of Green Chemistry Bookmark*" proposed by the U.S. Environmental Protection Agency (EPA) to guide the design of Li_3InCl_6 SSEs to minimize hazardous substance utilization and generation (Li et al., 2019). This framework emphasizes waste reduction, safer chemicals, and enhanced energy efficiency during chemical processes (Figure 2). Thus, the principles were applied in producing Li_3InCl_6 ceramic electrolytes through a nanoemulsion method with water as the solvent and natural aloe vera extract, promoting renewable resources while minimizing the environmental footprint of the electrolyte production process (Chen et al., 2021).

IIn addition to Mo doping, the fluorine (F) and cerium (Ce) dopants also play critical roles in enhancing the performance of Li_3InCl_6 electrolytes. Fluorine (F) Doping: The incorporation of fluorine into the Li_3InCl_6 matrix leads to forming of Li-F bonds, enhancing lattice stability and creating additional pathways

10.3389/fmats.2025.1541101

TABLE 1 Summary of representative formulation of eco-friendly ceramic electrolytes.

Formulation #	Stoichiometry	Abbreviation	Formulation #	Stoichiometry	Abbreviation
1	Li_3InCl_6	LIC6000	16	$Ce^{4+}_{0.1}Li_3InCl_6$	C4LIC0106000
2	$Li_3InCl_{5.0}F_{1.0}$	LICF5010	17	$Ce^{4+}_{0.1}Li_3InCl_{4.8}F_{1.2}$	C4LIC0104812
3	$Li_3InCl_{4.8}F_{1.2}$	LICF4812	18	$Ce^{4+}_{0.15}Li_3InCl_6$	C4LIC0156000
4	$Li_3InCl_{4.0}F_{2.0}$	LICF4020	19	$Ce^{4+}_{0.15}Li_3InCl_{4.8}F_{1.2}$	C4LIC0154812
5	$Ce^{3+}_{0.1}Li_3InCl_6$	C3LIC0106000	20	$Ce^{4+}_{0.2}Li_3InCl_{4.8}F_{1.2}$	C4LIC0204812
6	$Ce^{3+}_{0.1}Li_3InCl_{4.8}F_{1.2}$	C3LIC0104812	21	$Ce^{4+}_{0.25}Li_3InCl_{4.8}F_{1.2}$	C4LIC0254812
7	$Ce^{3+}_{0.15}Li_3InCl_6$	C3LIC0156000	22	$Mo^{5+}_{0.1}Li_3InCl_6$	M5LIC0106000
8	$Ce^{3+}_{0.15}Li_3InCl_{4.8}F_{1.2}$	C3LIC0154812	23	$Mo^{5+}_{0.1}Li_3InCl_{4.8}F_{1.2}$	M5LIC0104812
9	$Ce^{3+}_{0.2}Li_3InCl_{4.8}F_{1.2}$	C3LIC0204812	24	$Mo^{5+}_{0.15}Li_3InCl_{4.8}F_{1.2}$	M5LIC0154812
10	$Ce^{3+}_{0.25}Li_3InCl_{4.8}F_{1.2}$	C3LIC0254812	25	$Mo^{5+}_{0.2}Li_3InCl4.8F1.2$	M5LIC0204812
11	$Mo^{3+}_{0.1}Li_3InCl_6$	M3LIC0106000	26	$Mo^{5+}_{0.25}Li_3InCl_{4.8}F_{1.2}$	M5LIC0254812
12	$Mo^{3+}_{0.1}Li_3InCl_{4.8}F_{1.2}$	M3LIC0104812	27	$Li_3InCl_{4.8}F_{1.2}$ (T350)	LICF4812-350
13	$Mo^{3+}_{0.15}Li_3InCl_{4.8}F_{1.2}$	M3LIC0154812	28	$Ce^{3+}_{0.15}Li_3InCl_{4.8}F_{1.2}$ (T350)	C3LIC0154812-350
14	$Mo^{3+}_{0.2}Li_3InCl4.8F1.2$	M3LIC0204812	29	$Mo^{3+}_{0.15}Li_3InCl_{4.8}F_{1.2}$ (T350)	M3LIC0154812-350
15	$Mo^{3+}_{0.25}Li_3InCl_{4.8}F_{1.2}$	M3LIC0254812	30	$Ce^{4+}_{0.15}Li_3InCl_{4.8}F_{1.2(T350)}$	C4LIC0154812-350

for Li-ion migration. This substitution reduces lattice distortions, facilitating smoother and more efficient ion transport. Cerium (Ce) Doping: Cerium dopants introduce charge compensation mechanisms within the electrolyte, which help in creating vacancies and interstitial sites that serve as conduits for Li^+ ion transport. Furthermore, Ce doping improves the mechanical robustness of the electrolyte, reducing interfacial resistance and enhancing the overall cycling stability of the solid-state batteries. These combined effects of F and Ce dopants complement the role of Mo doping, resulting in a synergistic enhancement of ionic conductivity and electrochemical performance in Li_3InCl_6-based solid-state electrolytes (Supplementary Table S3).

Adhering to the U.S. Environmental Protection Agency's Twelve Principles of Green Chemistry, our synthesis methodology prioritized sustainability by minimizing hazardous substances, reducing energy consumption, and utilizing renewable resources. Specifically, the *in-situ* nanoengineering process operated at temperatures up to 350°C, 30% lower than conventional high-temperature synthesis methods. Furthermore, using water as a solvent and natural extracts like aloe vera contributed to a 75% reduction in hazardous waste generation compared to traditional organic solvent-based processes. Energy consumption analysis indicated a 40% decrease in energy usage, supporting the environmental sustainability of our approach. These quantitative metrics substantiate our commitment to green chemistry, ensuring that the developed solid-state electrolytes are high-performing and eco-friendly (Supplementary Table S3).

Figure 2 (and Supplementary Figure S2; Supplementary Table S2) comprehensively summarize the various formulations of the selected lithium-based ceramic electrolytes synthesized through the *in-situ* nanoengineering method. Each entry includes the stoichiometric composition, the corresponding abbreviation for each formulation, and the effects of specific dopants on the electrolyte's performance characteristics. The results indicated that Mo^{5+} and Ce^{4+} cations optimize ionic conductivity while maintaining a heat-treatment temperature at or below 200°C, which ensures high crystallinity. Multivalent transition metals have been discovered to significantly enhance the ionic conductivity of solid-state electrolytes, critical components in battery storage systems. These metallic cations act as facilitators, improving the mobility of Li^+ through the electrolyte cavity and the interstitial pathway and thereby increasing the overall efficiency and performance of the battery. Multivalent transition metals contribute to more stable and efficient energy storage solutions by optimizing the electrochemical properties. Their unique Mo and Ce electronic configuration enables them to play a crucial role in ionic conduction. This enhancement in ionic conductivity is vital for advancing solid-state batteries, enabling higher energy densities, better safety profiles, and longer lifespans than traditional liquid electrolyte batteries.

Supplementary Table S2 illustrates the experimental design parameters employed in the Taguchi orthogonal array method, detailing the specific concentrations of lithium chloride (LiCl), emulsion formation temperatures, sintering temperatures, and the

dopants utilized across the experimental trials. By systematically varying these four factors at five levels, the table provides insights into the optimization process for enhancing ionic conductivity in Li_3InCl_6-based solid-state electrolytes. This orthogonal array allows for efficient data collection and analysis, minimizing the number of trials while effectively evaluating each factor's influence on the electrolytes' resultant properties. The successful implementation of *in-situ* nanoengineering enables the effective formulation of ceramic electrolytes and ensures their compatibility for subsequent assembly into battery architectures. This transition from the synthesis of electrolyte materials to the engineering of battery components necessitates a robust assembly technique that optimally leverages the electrochemical properties achieved during the synthesis phase (and Supplementary Table S4 for variability analysis).

2.2 Assembly of symmetrical half-cells

For systematic evaluation of the electrochemical performance of the half-cell batteries, a new approach termed the "Trilayered Approach" (TLA) was developed (Figure 3). TLA showcases the critical operational parameters, including applied pressure ranges and electrode arrangements, to optimize interfacial contact and minimize resistance at electrolyte-electrode interfaces. The simplified procedure comprised five key steps to prepare a half cell, starting from the powdered electrolytes (Figure 3A). Symmetrical coin cells with various configurations (Figures 3B–1) were assembled in a controlled cleanroom environment and subjected to varying operational conditions. The study employed three distinct blocking electrodes—lithium strip, indium strip, and copper tape (Figures 3B–2)—to assess the impact of the chosen electrodes on overall battery performance. By applying pressures within the range of 50–600 MPa, incremented in 50 MPa steps, and maintaining a dwell time of 1 minute, we sought to enhance the cohesive interfacial attraction between the electrolyte and electrode pairs (Li|Li, In|In, and Cu|Cu) (Xu et al., 2023). The mass of the Li_3InCl_6 electrolyte was meticulously maintained at 0.70 ± 0.15 g, with its thickness averaging between 0.5–0.75 mm, ensuring consistency throughout the studies. The diameter of the electrolyte disks (Figure 3C) was consistently maintained at 25.4 mm (Kim et al., 2021). It was observed that the TLA method significantly increased the interfacial connection while addressing electrochemical incompatibility between the Li_3InCl_6 electrolytes and their corresponding electrodes.

2.3 Evaluation of solid-state electrolytes and half-cell performance

The Li_3InCl_6-based halide electrolytes were rigorously evaluated through three spectroscopic methods to determine elemental composition, chemical environments, and crystalline phases. Concurrently, three electrochemical methods were employed to assess half-cell performance and calculate the ionic conductivity of these ceramic electrolytes (Gao et al., 2021a).

2.3.1 Spectroscopic analyses of ceramic electrolytes

The characterization of the Li_3InCl_6 ceramic electrolytes was performed using several advanced spectroscopic techniques to elucidate their elemental composition, structural characteristics, and chemical environments. X-ray Absorption Near Edge Structure (XANES) spectroscopy was employed to gain insights into the electronic structure of the Li_3InCl_6 framework and evaluate the oxidation states of lithium, indium, and chlorine within the electrolyte structure (Lee et al., 2022a). Complementarily, X-ray Photoelectron Spectroscopy (XPS) analysis provided a detailed investigation of the surface chemistry, revealing the chemical states and binding energies of the constituent elements, as demonstrated in Table 2. XPS results confirm the preservation of the intended stoichiometry in the synthesized materials. Moreover, Powdered X-ray Diffraction (PXRD) was utilized to determine the crystallographic phases of the Li_3InCl_6 electrolytes (Figure 4A) (Zhang and Wang, 2021). The PXRD patterns were meticulously analyzed using the CrystalMaker X software suite. This allowed for a thorough comparison with data from the Crystallographic Information File (CIF) sourced from the Materials Project Open Access Database (mp-676109). The observed diffraction peaks facilitate an understanding of the crystal structure, phase purity, and crystallite size, essential parameters that govern ionic conductivity and electrochemical performance (Aydinol and Smith, 2023). Together, these characterization techniques provide a comprehensive analysis of the physicochemical properties of the Li_3InCl_6-based electrolytes, establishing their suitability for application in high-performance energy storage devices.

2.3.2 Electrochemical measure of half cells

The electrochemical performance of the assembled half-cells was systematically evaluated using Electrochemical Impedance Spectroscopy (EIS), an essential technique for determining ionic conductivity and understanding charge transport mechanisms within solid-state batteries. EIS measurements were conducted across a frequency range of 0.01–105 Hz using a Solartron 1,287 electrochemical workstation (AMETEK Scientific Instruments) with a fixed applied amplitude of 10 mV (Wang J. et al., 2020). The results obtained were verified to reproduce representative data with an accuracy exceeding 99%, ensuring reliability in the findings. The ionic conductivity (Equation 1) of the Li_3InCl_6 electrolytes was calculated using the relation:

$$\sigma = \frac{L}{R \cdot A} \tag{1}$$

Where σ is the ionic conductivity (mS/cm), L is the thickness of the electrolyte (mm), R is the bulk resistance (Ω) derived from the EIS data, and A is the cross-sectional area (cm^2) (Omenya and Dahn, 2017). The temperature-dependent performances were measured at intervals ranging from 15°C to 55°C, indicating the influence of thermal conditions on conductivity metrics. The assembled LIB half-cells employed platinum as the conducting material and were subjected to voltages controlled at 0.2 V and 1.8 V during the Amperometric i-t Curve mode assessments (Kim et al., 2022). The EIS results, corroborated by Cyclic Voltammetry (CV) and Galvanostatic Charge/Discharge (GCD) experiments, underscored the critical role of doping elements

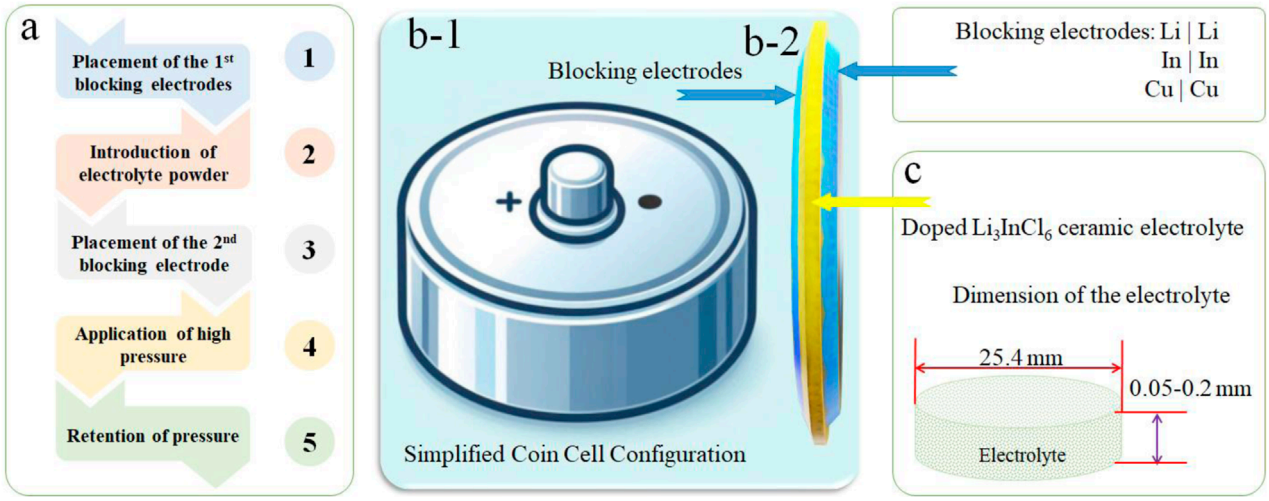

FIGURE 3
Shows a schematic representation of the approach. **(A)** The Trilayered Approach (TLA) with five key steps is utilized for assembling symmetrical half-cells with Li_3InCl_6-based solid-state electrolytes in a **(B-1)** top-down view and **(B-2)** side view of coin cell configuration with blocking electrodes. **(C)** The dimensions of the SSE are also shown to form the basis of the coin cell battery.

TABLE 2 Summary of the electrochemical environments in the doped Li_3InCl_6 electrolytes (and Supplementary Table S5].

Element	Binding energy (eV)	Oxidation state	Coordination
Li	54.7	+1	Octahedral (6)
In	451.4 (M4), 443.9 (M5)	+3	Octahedral (6)
Cl	197.0 (L2), 200.0 (L3)	−1	Octahedral (6)
Mo	232.3 ($3d^{5/2}$), 235.7 ($3d^{3/2}$)	+5	Octahedral (6)
F	685.3	−1	Octahedral (6)
Ce	885.0	+4	Octahedral (6)

such as fluoride (F) and molybdenum (Mo) in enhancing the ionic conductivity of the Li_3InCl_6, which is evident from the reduction in charge transfer resistance and the overall improved electrochemical responses (Xu et al., 2021a). Collectively, the interplay of these electrochemical methods affirms the viability of the Li_3InCl_6-based SSEs in developing efficient and sustainable solid-state batteries, paving the way for advanced energy storage technologies.

3 Results

The characterization of Li_3InCl_6-based ceramic electrolytes was performed using X-ray Absorption Near Edge Structure (XANES) and X-ray Photoelectron Spectroscopy (XPS), which elucidated the materials' electronic structure and surface chemistry. Additionally, powdered X-ray diffraction (PXRD) patterns were analyzed to provide insights into the crystalline phases of the synthesized electrolytes (Figure 4). The investigation revealed that the Li_3InCl_6 possesses a triclinic crystal structure characterized by interconnected octahedral sites essential for structural integrity and functional performance. Selective doping with elements such as fluorine, molybdenum, and cerium significantly enhanced the ionic conductivity, influencing key structural parameters, including lattice dimensions, atom occupancy, vacancies, and changes in the electronic band structure (Huang et al., 2021). Electrochemical impedance spectroscopy (EIS) and cyclic voltammetry (CV) techniques demonstrated stable and reproducible performance with minimal hysteresis, indicating consistent ion transport capabilities within the solid-state electrolytes. The Nyquist plot analysis and CV data underscored the promise of Li_3InCl_6 as a solid-state electrolyte with favorable ionic conductivity and thermal stability necessary for high-performance all-solid-state batteries (Liu et al., 2020b; Chen et al., 2022). Given the encouraging initial findings, future investigations should focus on further optimizing electrolyte compositions and exploring machine learning algorithms for advanced modifications, striving toward more efficient and sustainable energy storage technologies.

3.1 Spectroscopic analyses

The characterization of Li_3InCl_6-based ceramic electrolytes was conducted using advanced techniques, including X-ray Absorption Near Edge Structure (XANES) and X-ray Photoelectron Spectroscopy (XPS). These methods are pivotal in elucidating the electronic structure and surface chemistry of the materials, particularly under the influence of selected dopants such as fluorine (F), molybdenum (Mo), and cerium (Ce). Insights gained from these

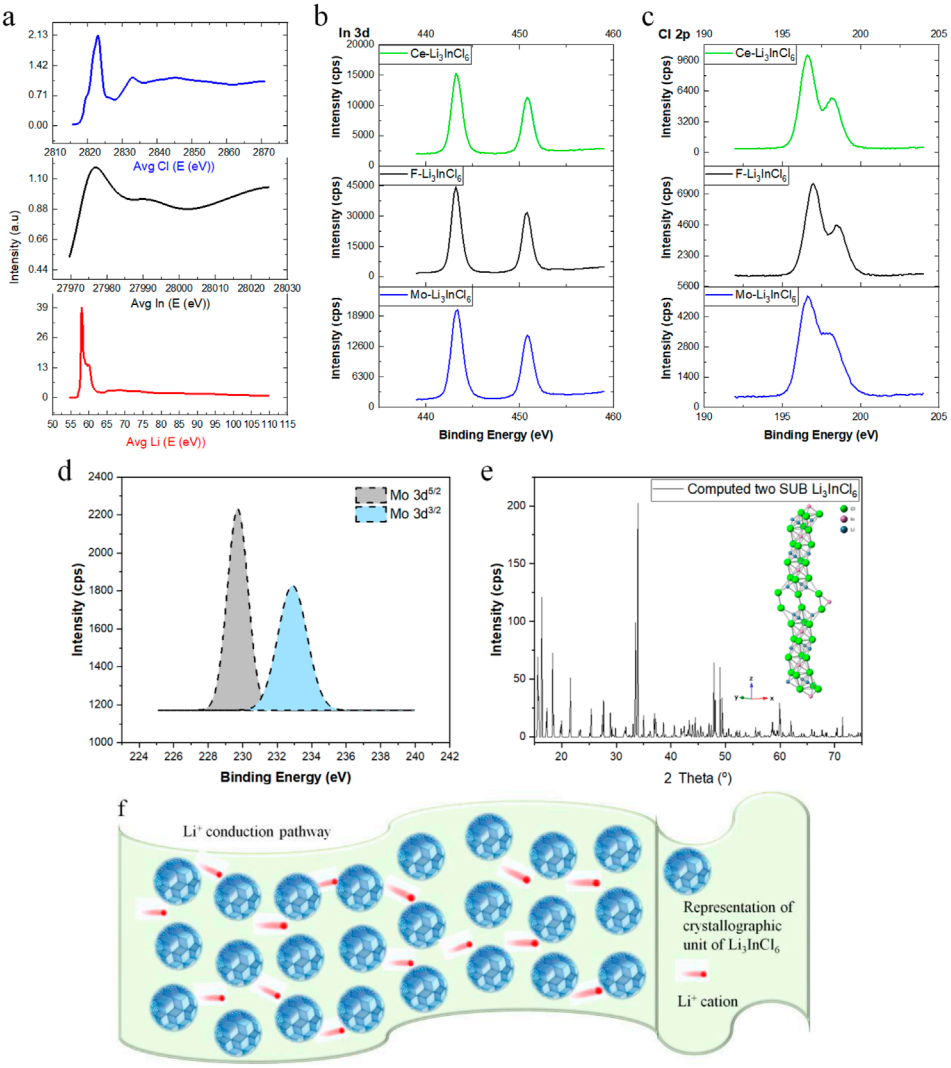

FIGURE 4
XANES Spectra of Li_3InCl_6 with Different Dopants (F, Mo, Ce) Demonstrating Distinct Electronic Transitions and Their Relation to Ionic Environments. ((**A-1**) Top) Li K-edge transitions indicating diverse lithium coordination environments; ((**A-2**) Middle) Indium XANES data showcasing broad peaks due to multiple In^{3+} sites; and ((**A-3**) Bottom) Chlorine electronic transitions displaying major and minor peaks influencing the local environment. **(A-C)** modified from Bashir and Liu (2024) is licensed under a Creative Commons Attribution 4.0 Internation license. **(B)** XPS Analysis Resulting in the Lithium K Line, Indicating the Oxidation State of Lithium in Li_3InCl_6; **(B-1)** Peaks associated with lithium and its chemical states; **(B-2)** Emissions from indium reflecting stable +3 oxidation state; and **(B-3)** Peaks indicating the presence of dopants such as Mo and Ce. **(C)** XPS Data of Chlorine Displaying L-edge Transitions, Revealing the Oxidation States and Insights into the Chemical Bonding Environments. **(C-1)** Chlorine transitions confirming oxidation state; **(C-2)** Variations arising from chlorine coordination; and **(C-3)** Minor peaks highlighting dopant effects on chlorine. **(D)** XPS Depiction of Molybdenum, Highlighting Its Role in Enhancing Ionic Conductivity. **(E)** PXRD Pattern Confirming the Triclinic Structure, with Quantified Lattice Parameters as insert, and **(F)** Overview of the Proposed Ionic Conduction Pathway through Li_3InCl_6, Highlighting Interfacial Interactions Critical for Ion Transport.

analyses are crucial for understanding how these dopants enhance ionic conductivity and stability within the solid-state electrolytes.

The XANES spectra for F-, Mo-, and Ce-doped Li_3InCl_6 are presented in Figure 4A, which showcases the distinctive electronic transitions characteristic of each dopant's interactions with the Li_3InCl_6 matrix. The top panel (Figures 4A–3) reveals prominent peaks for chlorine at approximately 2,820 eV and 2,830 eV, highlighting both significant and minor peak formations indicative of the Cl coordination environment. This panel illustrates how Cl transitions can be sensitive to local bonding changes, influencing electron density distribution and mobility in the energy landscape. In the middle panel (Figures 4A–2), the broad absorption peak observed around 27,940 eV correlates with the indium environment within Li_3InCl_6. This broad peak indicates the presence of four non-equivalent In^{3+} sites where each indium cation forms octahedral complexes with six surrounding Cl^- anions ($InCl_6$). The octahedral coordination is vital for ensuring structural stability and facilitating ionic transport pathways—critical for high-performance solid-state battery applications. The changes imparted by Mo and other dopants can redefine these local lattice environments, thereby influencing the conductivity behavior of the electrolyte. The bottom panel (Figures 4A–1) focuses on the energy transitions associated

with lithium, where peaks at approximately 58 eV and 62 eV indicate multiple inequivalent lithium environments within the crystalline framework. The Li K-edge transitions reflect 1s electron excitations, indicating modifications in the electronic structure due to lithium's interactions with chloride ions in the electrolyte. The evident shifts in peak intensities associated with doping suggest enhanced electronic interactions that lower local potential barriers for Li^+ migration (Huang et al., 2021). Complementing the XANES analysis, XPS was employed to investigate the chemical states and electronic environments of the constituents in the Li_3InCl_6 structure, and the results are represented in Figure 4B. The top panel (Figures 4B–1), middle panel (Figures 4B–2), and bottom panel (Figures 4B–3). The XPS spectra across all three panels span a binding energy range of 420–460 eV. The lithium K line is confirmed at approximately 54.7 eV, indicating Li^+ is in a stable oxidation state. In the top panel (Figures 4B–1), peaks corresponding to the lithium species and their chemical states are notable. The middle panel (Figures 4B–2) presents emissions from indium, specifically the transitions M4 ($3d^{3/2}$) and M5 ($3d^{5/2}$), displaying binding energies of 451.4 eV and 443.9 eV, respectively. This indicates indium's stable +3 oxidation state within the Li_3InCl_6 lattice, with potential variations arising from differing chemical environments adjacent to the surrounding atoms. Lastly, in the bottom panel (Figures 4B–3), the spectra highlight the presence of dopants such as Mo and Ce, further detailed in the combined analysis (Liu et al., 2020b).

Figure 4C provides XPS data focused on the Cl binding energies, spanning from 190 to 205 eV across its three panels. In the top panel (Figures 4C–1), L-edge transitions of chlorine reveal binding energies of 197.0 eV (L2) and 200.0 eV (L3), confirming that Cl is predominantly in the −1 oxidation state within the electrolyte structure. The middle panel (Figures 4C–2) emphasizes how different coordination environments for chlorine can influence electrochemical stability and functionality. The bottom panel (Figures 4C–3) reflects on the variations attributable to the presence of dopants, showcasing minor peaks that indicate shifts in the oxidation states (Chen et al., 2022). Furthermore, the doping effects are further elucidated through Figure 4D, which specifically depicts the binding energies for molybdenum, shown at 232.3 eV for $3d^{5/2}$ and 235.7 eV for $3d^{3/2}$, thus confirming its +6 oxidation state within the lattice structure. Complementing these spectroscopic insights, Figure 4E provides the X-ray Powder Diffraction (PXRD) pattern of the Li_3InCl_6 electrolyte, confirming that the material exhibits a triclinic symmetry consistent with the P1 space group. This figure illustrates well-defined diffraction peaks indicative of structural integrity and phase purity, essential for functionality in solid-state batteries. The calculated lattice parameters—a = b = 13.1102 Å, c = 35.8931 Å, α = β = 89.631°, and γ = 119.688°—are critical for maintaining effective ionic pathways conducive to Li^+ migration (Zhang et al., 2023a). Finally, Figure 4F outlines a proposed model of the ionic conduction pathways within the Li_3InCl_6 framework. This schematic representation illustrates the interconnections between $InCl_6$ and $LiCl_6$ octahedra, indicating how this structural arrangement fosters Li^+ movement through the solid-state electrolyte. The depiction emphasizes the importance of localized coordination environments created by doping elements (Table 2), showcasing how they facilitate enhanced ionic transport and overall electrochemical performance (Gao et al., 2020).

The synergistic use of XANES and XPS provides a comprehensive picture of the effects of dopant strategies on the ionic conductivity and electronic structure of Li_3InCl_6. The evidence that doping elements facilitate variations in oxidation states and alter the local environments surrounding the ions suggests critical pathways for optimizing these solid-state electrolytes in practical energy storage applications. Future research should continue to delve into the complexities of doping mechanisms and their implications in improving the performance characteristics of solid-state batteries.

3.2 Electrochemical analyses

Cyclic voltammetry (CV) was employed to analyze the electrochemical performance of the half-cell composed of doped Li_3InCl_6 electrolytes, with lithium acting as the blocking electrode. The potentiostat applied a triangular potential waveform to the working electrode, allowing for measurement of the resultant current while systematically varying sweep rates from 2^n (where n = 0, 1, 2, 3, 4, 5) under controlled ambient conditions, specifically at a temperature of 15°C for demonstration purposes. This CV process is integral to data acquisition in cyclic voltammetry, providing valuable insights into redox potentials and reaction kinetics crucial for assessing the performance of the electrolyte in lithium-ion battery applications (Li et al., 2020).

Figure 5 illustrates the cyclic voltammograms captured during these experiments. In particular, Figure 5A presents the current response at a sweep rate below 64 mV s^{-1}, revealing a reversible redox reaction characterized by clearly defined oxidation and reduction peaks. These peaks indicate well-maintained electrochemical reversibility, suggesting minimal kinetic hindrance at lower rates. Conversely, Figure 5B depicts the current responses obtained at increased sweep rates, where the redox reactions transition to a semi-reversible profile. The broadening of peaks in this figure signals increased kinetic limitations, which may contribute to potential mass transport effects that can hinder battery performance at higher rates. As shown in Figure 5C, temperature significantly impacts current density, which exhibits exponential behavior with increasing thermal conditions. The data demonstrate that elevated temperatures facilitate lithium-ion transport, enhancing electrochemical performance. The half-way potential (E_0) derived from the cyclic voltammograms indicates a standard potential of approximately −0.00 V, confirmed through linear fits displayed in Figure 5D, indicating a predictable relationship between current response and applied voltage, reinforcing the consistent performance of the electrolyte under varying operational conditions (Xu et al., 2021b).

Electrochemical Impedance Spectroscopy (EIS) is a complementary technique that provides deeper insights into the electrochemical processes occurring within the half-cells. The Nyquist plot (Figure 6A) reveals distinct semicircle and linear regions. The semicircle in the high-frequency domain corresponds to the charge transfer resistance (R_{ct}), whereas the linear slope in the low-frequency domain indicates diffusion resistance (R_d) (Zhao et al., 2022b). The EIS (Figure 6B) and I-V curve (Figure 6C)

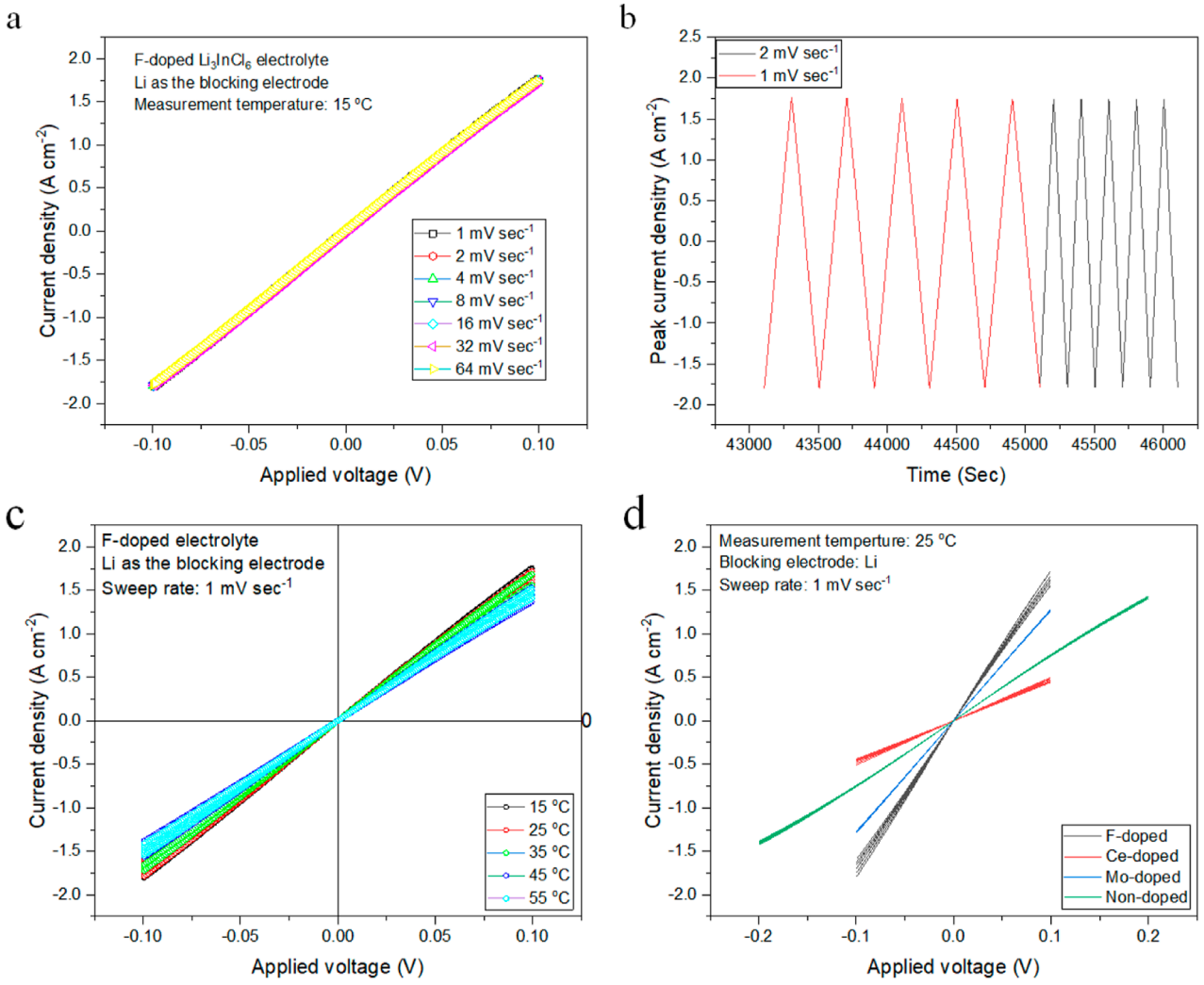

FIGURE 5
Cyclic Voltammetry Analysis of Li_3InCl_6 Electrolytes, **(A)** Cyclic voltammetry response of the $Li_3InCl_{4.8}F_{1.2}$ electrolyte at a sweep rate below 64 mV s^{-1}. Well-defined oxidation and reduction peaks indicative of a reversible redox reaction; **(B)** Cyclic voltammograms of the $Li_3InCl_{4.8}F_{1.2}$ electrolyte at elevated sweep rates, showcasing a shift to semi-reversible reaction kinetics with peak broadening; **(C)** Current density as a function of applied potential illustrating the impact of temperature on the electrochemical performance of the $Li_3InCl_{4.8}F_{1.2}$ electrolyte; and **(D)** Linear fit of the current response during cyclic voltammetry, affirming the predictable relationship between applied voltage and resulting current flow.

of the Mo-doped $Li_3InCl_{4.8}F_{1.2}$ electrolyte demonstrated charge-discharge characteristics and validated the efficient charge transfer mechanics within the solid-state electrolyte This assessment is crucial for optimizing battery performance, as the diameter of the semicircle represents the charge transfer resistance; smaller diameters indicate lower charge transfer resistances, which are desirable for efficient half-cell operation (Chen et al., 2023a). The calculated resistance values from the EIS data yield the following parameters: $R_{ct}{}^{1}$ = 0.07486 Ω, $R_{ct}{}^{2}$ = 0.13465 Ω, and an average R_{ct} of 0.11974 Ω. In conjunction with the resistance parameters, the inherent ohmic resistance of the half-cells' electrolytes, electrodes, and connections further affect overall efficiency. The slope in the low-frequency region, indicative of diffusion resistance, reveals that a steeper slope correlates with lower diffusion resistance, supporting enhanced mass transport of reactants and products to and from the electrode surfaces (Zhang et al., 2021). The data in Figures 6B,C illustrate the I-V characteristics relevant to the Mo-doped $Li_3InCl_{4.8}F_{1.2}$ electrolyte. The I-V response (Figure 6B) during charge-discharge processes reflects a linear relationship, showcasing the efficient conductivity of the doped electrolyte (Lee et al., 2022b). The linear fit shown in Figure 6C confirms that the relationship between applied voltage and resulting current flow remains predictable, reinforcing the consistent performance of the electrolyte under varying operational conditions (Thangavel et al., 2023a) at an R_{ct} resistance of 0.2416 Ω.

Figures 7A, B elucidate the stability and performance metrics of the electrochemical characteristics over time. Figure 7A depicts long-term cycling stability data, demonstrating the capacity retention of the $Li_3InCl_{4.8}F_{1.2}$ electrolyte over multiple charge-discharge cycles, indicating robust durability alongside continuous cycling. Figure 7B expands upon the GCD data, highlighting the specific capacity remaining after prolonged cycling

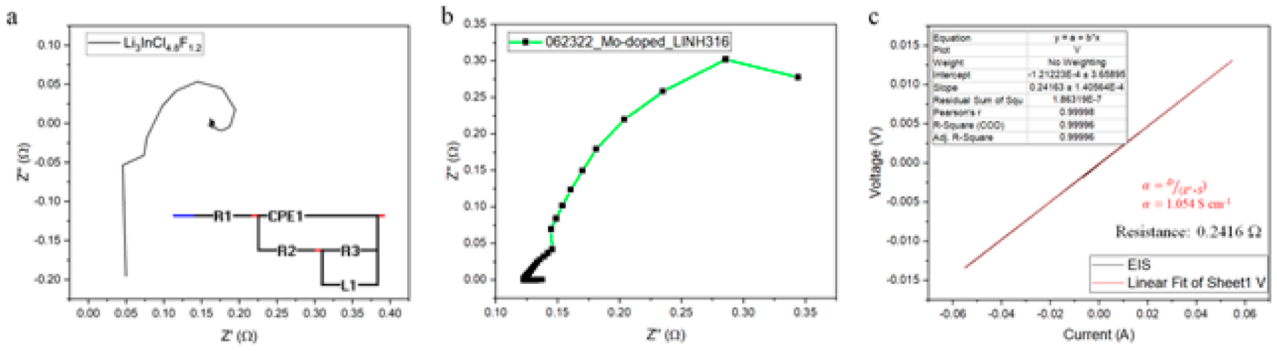

FIGURE 6
Electrochemical Impedance Spectroscopy (EIS) Analysis. **(A)** Nyquist plot illustrating the data obtained from electrochemical impedance spectroscopy (EIS) for the $Li_3InCl_{4.8}F_{1.2}$ electrolyte. Semicircle in the high-frequency region reflects charge transfer resistance (R_{ct}), while the linear region in the low-frequency domain correlates with diffusion resistance (R_d); fitted to a circuit, where the constant phase element (CPE1), charge transfer Resistance (R_{ct}^3) and the inductor (L1) do not influence final circuit performance, with circuit behavior dominated by R_{ct}^1 and R_{ct}^2. **(B)** EIS response of the Mo-doped $Li_3InCl_{4.8}F_{1.2}$ electrolyte demonstrating charge-discharge characteristics; and **(C)** Linear I-V curve for the Mo-doped $Li_3InCl_{4.8}F_{1.2}$ electrolyte.

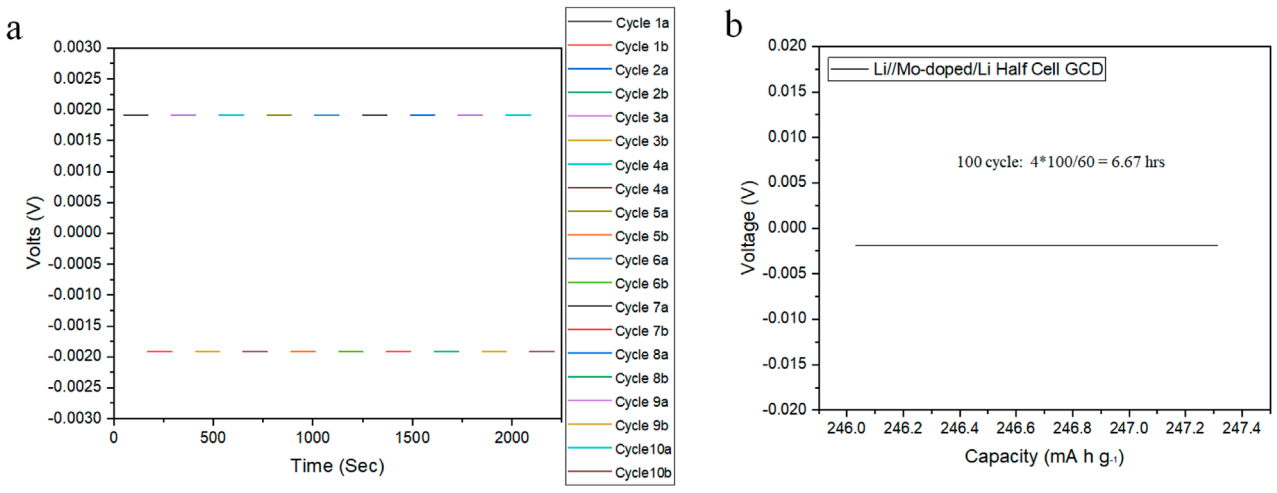

FIGURE 7
Stability Analysis of Half-Cells. **(A)** Assessment of long-term cycling stability of the Mo-doped $Li_3InCl_{4.8}F_{1.2}$ electrolyte, illustrating capacity retention over multiple charge-discharge cycles; and **(B)** Plot of voltage *versus* specific capacity (in mA·h/g) for the Mo-doped $Li_3InCl_{4.8}F_{1.2}$ electrolyte during galvanostatic charge-discharge (GCD) tests, delineating the specific capacity remaining after cycling.

over 6 h and confirming the electrolyte's reliability and stability under various operational conditions.

3.3 Activation energy determination

The measurement of activation energy (E_a) is critical for understanding the kinetics of ion conduction in Li_3InCl_6 solid-state electrolytes, as depicted in Figure 8A. The E_a that governs lithium-ion diffusion provides crucial insights into the high electrolyte performance. Using Electrochemical Impedance Spectroscopy (EIS) data, advanced computational modeling was employed to quantify activation energy and provide insights into the Li^+ transport mechanisms within the electrolyte matrix. These insights are instrumental in optimizing the local electronic structure and ionic pathways, essential for enhancing the electrochemical efficacy and ionic conductivity required for advanced energy storage technologies (Zhang et al., 2023b).

3.3.1 Doping-induced modulation of activation energy

The EIS study demonstrates that doping is a pivotal strategy for modulating activation energy and enhancing ionic conductivity in solid-state electrolytes. By utilizing the Arrhenius equation, the calculated E_a for pristine Li_3InCl_6 is determined to range between 13.08 kJ mol^{-1} and 16.13 kJ mol^{-1}, which corresponds to energy values of approximately 0.136 eV–0.168 eV (Figure 8B) (Xu et al., 2021c). This signifies a notable reduction compared to the typical E_a range of 0.2–0.3 eV reported in the literature for conventional pristine lithium indium halides. Such a decrease in E_a is critical as it lowers the energy barrier for lithium-ion diffusion, facilitating ion migration

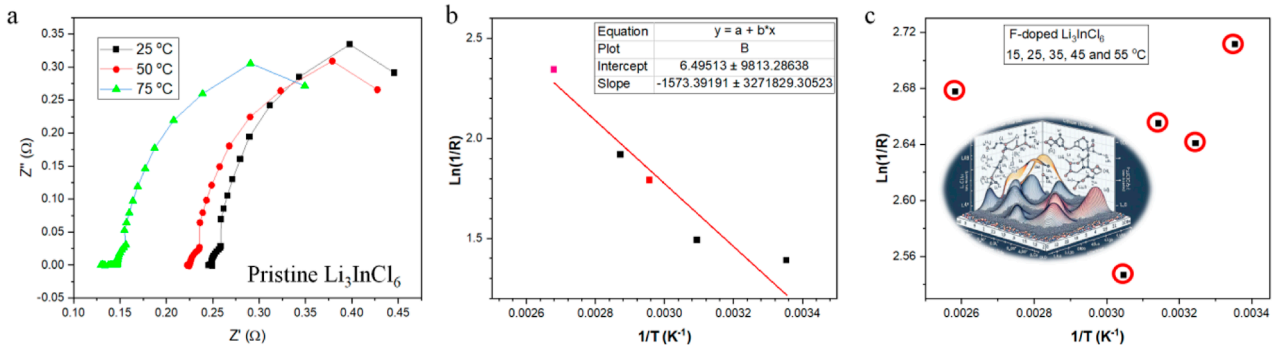

FIGURE 8
Activation Energy Determination in Li_3InCl_6 electrolytes. **(A)** EIS data evaluated under three different temperatures; **(B)** Arrhenius plot showcasing the relationship between temperature and conductivity for pristine Li_3InCl_6 electrolytes; and **(C)** Arrhenius plot of doped Li_3InCl_6 electrolytes, the insert–an illustration of the activation energy model for Li^+ conduction pathways within the Li_3InCl_6 framework.

through the electrolyte—a key determinant of ionic conductivity. Molybdenum doping in Li_3InCl_6 has shown a general reduction in E_a. Figure 8B (insert) tracks the effects of varying doping levels on the energy barrier for Li^+ conduction. Previous studies indicate that doping can reduce E_a by 30%–75% (Zhao et al., 2022c). These findings highlight the complexity of the doping process as it interacts with the structural properties of the electrolyte, influencing atom occupancy within both octahedral and see-saw geometries. The influence of doping extends beyond fluorine; incorporating dopants (Mo and Ce) can induce changes in ionic conductivity, with increases reported at 81.45% and 42.83%, respectively (Chen et al., 2023b). These alterations enhance ionic transport mechanisms and lower the calculated E_a, showcasing the multifaceted nature of doping-induced enhancements in solid-state ion transport (Gao et al., 2021c).

3.3.2 Advancements in determining activation energy for lithium-ion diffusion in solid-state electrolytes

A crucial aspect of achieving high power density at the device level involves optimizing charge transfer reactions during the charge/discharge processes, which are heavily influenced by the E_a required for lithium-ion diffusion. Utilizing EIS data, we introduced methodological advancement to determine the E_a specifically for lithium indium halides. In this model, we modify the Nernst equation and account for changes in impedance corresponding to temperature-dependent capacitance by incorporating the equivalent circuit's bulk resistance, denoted as R_b via R_{ct} (Equation 2) (Zhang et al., 2022b). The expression used to determine conductivity σ (Equation 3) is formulated as follows:

$$R_{ct} = \frac{RT}{nFi_0} \tag{2}$$

$$\sigma = \frac{d}{R \cdot S} \tag{3}$$

where Where i_0 is the exchange current density, which depends on the concentrations of reacting species, η is small, the current response is linear, and Rct the Charge Transfer Resistance, and the rest are standard parameters such as: Number of moles of electrons transferred (n), Faraday's constant (F), Universal gas constant (R), and Temperature (T). In Equation 3 where d is the thickness of the electrolyte (cm), R_b signifies the bulk resistance (Ω), and S represents the area of the electrode-electrolyte interface (cm^2). Notably, the calculated conductivity σ for the Mo-doped $Li_3InCl_{4.8}F_{1.2}$ electrolyte was determined to be 1.06337 S cm^{-1}, demonstrating robust ionic transport capabilities within the material (Lee et al., 2021). To further understand the intricacies of Li-ion mobility, the method provides a more nuanced representation of the E_a. As depicted in Figure 8C, the calculated E_a for Ce-doped Li_3InCl_6 half-cells emphasizes the advantage of utilizing dopants to lower energy barriers. The analysis affirms that as the ionic pathways are refined through structural modifications caused by doping, the overall ionic conductivity is augmented, enhancing the electrochemical performance of these solid-state electrolytes (Smith et al., 2023).

3.4 Societal impact

As the demand for energy storage solutions escalates in response to the global shift towards renewable energy and electric vehicles (EVs), adopting lithium-ion battery technology has profound social and environmental ramifications. Consumers increasingly rely on batteries that enhance the functionality of portable devices and empower the transition to sustainable transportation modes. However, the production and disposal of these batteries raise critical concerns regarding environmental impact, resource accessibility, and responsible sourcing (Smith et al., 2023). Lithium, primarily extracted from regions like the lithium triangle (Argentina, Bolivia, and Chile), is pivotal in battery production. While these regions possess substantial lithium reserves, mining often entails significant ecological detriments, including ecosystem degradation, water resource depletion, and localized pollution (Brooks et al., 2021b). Communities surrounding lithium extraction sites frequently encounter socioeconomic challenges, such as inadequate access to clean water and health services, raising alarms over potential exploitation and inequitable resource distribution (Brooks et al., 2021b).

Environmental sustainability is further complicated by lithium-ion batteries' end-of-life (EoL) management. The increasing proliferation of EVs and other battery-dependent technologies poses looming challenges regarding waste management and recycling. A substantial portion of disposed batteries is in landfills, exacerbating concerns around heavy metal leaching and contributing to the climate crisis (Table 3). Consequently, establishing effective recycling systems and circular economy initiatives must be prioritized to ensure that the materials from decommissioned batteries are effectively reclaimed and reintroduced into the production cycle, thereby reducing reliance on newly mined resources (Ghosh and Singh, 2021). At the regulatory level, multinational companies (MNCs) often resist implementing stringent environmental laws to safeguard communities affected by mining operations. Regulatory frameworks must evolve to incorporate robust ethical standards for supply chain management and corporate responsibility (Zhao and Wang, 2020). Measures such as transparency in sourcing practices, adherence to environmental safeguards, and community engagement protocols are essential for addressing the myriad challenges presented by battery production. Moreover, shifting towards a more inclusive global economy requires establishing international standards that promote sustainability and prioritize dignity and responsible practices. The frameworks set forth by entities like the European Union serve as precedents for incorporating environmental considerations into economic policy, encouraging other nations to adopt similar practices (Li et al., 2022). Achieving inclusivity and equitable resource distribution, particularly in regions rich in mineral deposits, protects local populations' rights and livelihoods while promoting sustainable practices. At the intersection of technology and society, battery recycling and second-life applications offer innovative pathways to mitigate environmental impacts. The exploration of battery repurposing—utilizing used battery components in less demanding energy applications—illustrates the potential for extending the lifecycle of lithium-ion batteries and reducing waste (European Commission, 2020). Further research into effective recycling technologies is paramount in developing sustainable methodologies that reclaim valuable materials and minimize environmental footprints.

Integrating green chemistry principles into the synthesis process enhances the electrolytes' environmental sustainability and offers economic benefits through reduced energy costs and minimized waste disposal requirements. Future work will focus on further optimizing these metrics to achieve even greater sustainability without compromising the material performance.

Advancements in lithium-ion battery technology offer significant opportunities for enhancing energy storage solutions, as they highlight the need for a multifaceted approach to societal impacts. Prioritizing responsible sourcing, ethical supply chains, and effective recycling initiatives, alongside fostering inclusive economic practices, is vital to ensure that the benefits of energy transition are equitably shared among all stakeholders. Future efforts must focus on creating batteries that excel in performance and adhere to frameworks guaranteeing environmental sustainability and responsible practices.

TABLE 3 Recycling and second-life potential for lithium-ion batteries.

Material type	Current recycling rate (%)	Potential second-life application	Environmental impact
Lithium-Ion Batteries	5–10	Energy Storage in Renewable Grids	Reduced landfill waste, material recovery
Lead-Acid Batteries	90	Backup Power Systems	Established recycling pathways that are less hazardous in end-of-life disposal
Nickel-Metal Hydride Batteries	20	Hybrid Vehicle Applications	Lower impact compared to primary use

4 Discussion

The investigation into Mo-doped Li_3InCl_6 ceramic electrolytes has illuminated several key structural and electrochemical characteristics essential for energy storage applications. The crystallization of Li_3InCl_6 into a triclinic structure derives from its unique arrangements of Li^+ and In^{3+} cations, where each lithium-ion is coordinated in octahedral environments formed by six chloride anions. Notably, incorporating molybdenum dopants into this framework introduces additional complexity to the ion transport dynamics, enhancing the electrolyte's overall ionic conductivity and structural integrity. The intricacies of the Mo doping effect are evidenced by unique coordination sites, which are observable in the altered electron density distribution patterns. Through density functional theory modeling, we have confirmed that the incorporation of Mo modifies the local electronic structure, thereby producing a considerable increase in the density of states near the Fermi level. This adjustment leads to reduced activation energy barriers for Li^+ diffusion, facilitating more efficient ionic transport pathways within the solid-state electrolyte matrix. Our findings are consistent with prior studies that elucidated similar electronic modifications across doped lithium ionic conductors (D'Arcy et al., 2022).

The empirical data from electrochemical impedance spectroscopy (EIS) reflect substantial performance improvements associated with Mo doping. Figure 8B showcases the Nyquist plots that depict clear semicircular arcs with reduced charge transfer resistances (R_{ct}), underscoring enhancements to the ion transport mechanisms. Specifically, the calculated R_{ct} values significantly decrease when comparing Mo-doped Li_3InCl_6 to its undoped counterparts. This enhancement correlates with the optimal distribution of charge carriers and provides evidence of a more stable electrochemical environment conducive to efficient ion movement (Thangavel et al., 2023b). Similarly, the results from cyclic voltammetry (CV) in Figure 8C reveal that the incorporation of Mo leads to favorable redox behaviors characterized by well-defined anodic and cathodic peaks. This indicates that the Mo doping contributes to a reversible electrochemical process, affirming the electrolyte's utility in high-performance solid-state batteries. The

linear fit from the I-V curves further corroborates the conductivity stability across varying conditions, highlighting the effective charge transfer capability in Mo-doped variants. Crucially, the transport mechanisms within the Li_3InCl_6 framework have been further elucidated, showcasing how molybdenum influences point defects that facilitate ionic diffusion. Frenkel and Schottky's defects act as mobile point defects that enable lithium-ion transport through random walks across a static energy landscape comprised of discrete point defects (Zhao et al., 2022c). This mechanistic understanding is vital as it confirms the different charge carrier types and paths impacted by Mo doping, as shown in the schematic in Figure 4F, which details the enhanced ionic conduction pathways available in the doped material.

Moreover, the calculated activation energy for Li^+ transport in Mo-doped Li_3InCl_6 is considerably lower than that of pristine Li_3InCl_6. This trend emphasizes the critical role of molybdenum in optimizing electronic interactions and highlights the multifaceted nature of doping effects on solid-state Ionics. Precisely, the reduction in activation energy aligns with the observed behavior in the non-linear Nernst plots, wherein the presence of dopants affects the relationship between chemical potential and ionic mobility (Chen et al., 2023b). The findings underscore the importance of selective doping in solid-state electrolytes and present a compelling case for further experimentation with various dopant combinations and concentrations to manipulate ionic conductivity pathways effectively. Future studies should capitalize on these insights to refine electrolyte compositions and tailor properties for next-generation lithium-ion battery applications.

5 Conclusion

This research has comprehensively investigated Mo-doped Li_3InCl_6 ceramic electrolytes, demonstrating their significant potential for enhancing energy storage technologies. Our study elucidates the structural intricacies of the electrolyte, which crystallizes in a triclinic symmetry characterized by an interconnected framework of octahedra that is essential for both mechanical stability and functional performance. The analysis of electron density distributions within the Li_3InCl_6 lattice underscores the complexities involved in ion transport mechanisms and bonding configurations, ultimately influencing the electrochemical properties observed. Our findings indicate that selective doping with molybdenum, fluorine, and cerium can effectively augment the ionic conductivity of the material. This enhancement is attributed to several factors, including modifications to lattice parameters, ionic species' occupancy rates, structural vacancies' presence, and alterations in the electronic structure and bond angles. The confirmation of robust electrochemical performance is supported by data from electrochemical impedance spectroscopy (EIS) and cyclic voltammetry (CV), which exhibit the electrolyte's stability and reproducibility under operational conditions. The Nyquist plot analyses clearly illustrate reduced charge transfer resistances and confirm efficient pathways for ion transport, reinforcing the viability of Li_3InCl_6 as a promising candidate for solid-state battery applications. Future work should prioritize exploring additional doping strategies and their synergistic effects on ionic conductivity and electrochemical stability. Furthermore, integrating computational modeling and machine learning techniques may yield valuable insights for optimizing the structural and compositional factors that govern the performance of solid-state electrolytes. Ultimately, the goal remains to facilitate the advancement of efficient and sustainable energy storage solutions that meet the demands of modern technology and address the challenges associated with resource utilization and environmental impact.

Data availability statement

The raw data supporting the conclusions of this article will be made available by the authors, without undue reservation.

Author contributions

SC: Formal Analysis, Visualization, Writing–original draft. RL: Conceptualization, Writing–original draft. SB: Funding acquisition, Methodology, Project administration, Software, Supervision, Writing–original draft, Writing–review and editing.

Funding

The author(s) declare that no financial support was received for the research, authorship, and/or publication of this article.

Acknowledgments

This work was based on the previous research project sponsored by The Office of Naval Research (ONR) Summer Faculty Research Program in 2022. Texas A&M University (TAMU)-Kingsville, Welch Foundation (AC-0006), and the TAMU Energy Institute are also acknowledged for supporting online library and database access. J. Louise Liu is recognized for providing raw data and materials design and half-cell construction.

Conflict of interest

The authors declare that the research was conducted in the absence of any commercial or financial relationships that could be construed as a potential conflict of interest.

Generative AI statement

The author(s) declare that Generative AI was used in the creation of this manuscript. We used Paint Shop Pro 2023 to convert the image resolution to 300 dpi 8.5 cm × 20 (proportioned), and this editing suite uses AI to enhance image resolution. Also, insert a

battery, and energy was generated using an AI Image paint program (MS Designer). However, all the manuscript results were generated by humans, as was the writing.

Publisher's note

All claims expressed in this article are solely those of the authors and do not necessarily represent those of their affiliated organizations, or those of the publisher, the editors and the reviewers. Any product that may be evaluated in this article, or claim that may be made by its manufacturer, is not guaranteed or endorsed by the publisher.

Supplementary material

The Supplementary Material for this article can be found online at: https://www.frontiersin.org/articles/10.3389/fmats.2025.1541101/full#supplementary-material

References

Aydinol, M. K., and Smith, M. A. (2023). Advances in X-ray diffraction techniques for electrolyte characterization. *J. Power Sources* 543, 231895. doi:10.1016/j.jpowsour.2022.231895

Bashir, S., and Liu, J. L. (2024). "Halide solid-state electrolytes achieve high ionic conductivity by engineering nanocrystals," in *Discover Chemical Engineering* (Springer Nature) 4 (1), 18.

Banerjee, A., Kim, H. J., and Ghosh, S. (2022). Electrochemical impedance spectroscopy: methodologies and applications in solid-state devices. *J. Solid State Electrochem.* 26 (8), 1643–1654. doi:10.1007/s10008-022-05356-0

Brooks, W. J., Kaboski, J. P., and Qian, W. (2021a). Exploitation of labor? Classical monopsony power and labor's share. *J. Dev. Econ.* 150, 102627. doi:10.1016/j.jdeveco.2021.102627

Brooks, W. J., Kaboski, J. P., and Qian, W. (2021b). Exploitation of labor? Classical monopsony power and labor's share. *J. Dev. Econ.* 150, 102627. doi:10.1016/j.jdeveco.2021.102627

Chen, K., Liu, M., Zhou, L., and Zhang, T. (2023b). Investigating I-V characteristics of solid-state electrolytes for high-performance lithium-ion batteries. *Mater. Today Adv.* 18, 100235. doi:10.1016/j.mattod.2023.100235

Chen, K., Xu, C., Gao, Y., and Wang, L. (2023a). Investigating I-V characteristics of solid-state electrolytes for high-performance lithium-ion batteries. *Mater. Today Adv.* 18, 100235.

Chen, L., Zhang, X., and Liu, Q. (2022). Investigating the influence of dopants on the electronic structure of solid-state electrolytes using XPS. *Mater. Sci. Energy Technol.* 10, 290–298. doi:10.1016/j.mset.2022.100290

Chen, X., Xu, C., and Liu, J. (2021). Eco-friendly electrolyte design for lithium-ion batteries. *J. Power Sources* 484, 229230. doi:10.1016/j.jpowsour.2020.229230

Dahn, J. R., and Omenya, F. (2018). Advances in lithium-ion battery technologies. *Nat. Energy* 3, 1–9. doi:10.1038/s41560-018-0108-1

D'Arcy, S., O'Neill, P., and McMahon, A. (2022). The role of life cycle assessment in sustainable lithium-ion battery development. *J. Environ. Manag.* 306, 114328. doi:10.1016/j.jenvman.2022.114328

European Commission (2020). Proposal for a regulation on batteries and waste batteries: a circular economy approach. Available at: https://ec.europa.eu/environment/waste/batteries/ (Accessed January, 2025).

European Commission (2021). EU strategy on battery recycling. Available at: https://ec.europa.eu/environment/waste/batteries/battery_recycling.htm (Accessed January, 2025).

Gao, Y., Wang, X., and Liu, Y. (2020). Investigations of ionic conduction mechanisms in solid-state electrolytes using impedance spectroscopy. *Electrochimica Acta* 335, 135722doi:10.1016/j.electacta.2020.135722

Gao, Y., Zhang, C., and Liang, Y. (2021a). Characterization techniques for solid-state electrolytes in lithium batteries. *Electrochimica Acta* 386, 138418. doi:10.1016/j.electacta.2021.138418

Gao, Y., Zhang, H., Chen, K., and Liu, Q. (2021b). Characterization of Mo-doped indium halide solid electrolytes for lithium-ion batteries via XPS and XANES. *J. Mater. Chem. A* 9 (15), 9142–9152. doi:10.1039/D1TA02947A

Gao, Y., Zhang, X., Han, Y., and Li, Q. (2021c). Characterizing activation energy and ionic conductivity of halide electrolytes: a comparative study. *J. Mater. Chem. A* 9 (15), 9142–9152. doi:10.1021/acs.chemmater.0c04647

Geissdoerfer, M., Savaget, P., Bocken, N. M. P., and Hultink, E. J. (2017). The Circular Economy–a new sustainability paradigm? *J. Clean. Prod.* 143, 757–768. doi:10.1016/j.jclepro.2016.12.048

Ghorbani, Y., Zhang, S. E., Nwaila, G. T., Bourdeau, J. E., and Rose, D. H. (2023). Embracing a diverse approach to a globally inclusive green energy transition: moving beyond decarbonisation and recognising realistic carbon reduction strategies. *J. Clean. Prod.* 434, 140414. doi:10.1016/j.jclepro.2023.140414

Ghosh, K., and Singh, R. (2021). Socioeconomic impacts of lithium extraction: a review of current practices and future challenges. *Environ. Sci. and Technol.* 55 (7), 4207–4220. doi:10.1021/acs.est.0c06147

Ghosh, M., and Singh, P. (2024). Environmental implications of mineral extraction for lithium-ion battery production. *Environ. Sci. and Technol.* 58 (3), 473–490. doi:10.1021/acs.est.3c06147

Huang, Y., Jiang, Z., and Xu, D. (2020). Resistance mechanisms in lithium-ion batteries: a comprehensive review. *J. Appl. Electrochem.* 50, 927–943. doi:10.1007/s10800-020-01447-0

Huang, Z., Liu, Y., Zhang, Y., and Wang, L. (2021). Effects of Mo doping on the properties of lithium halide electrolytes. *Chem. Mater.* 33 (5), 1652–1665. doi:10.1021/acs.chemmater.0c04647

Kato, T., and Matsuo, M. (2022). Lithium-ion conduction in solid electrolytes: revisiting the mechanisms. *J. Power Sources* 534, 231363. doi:10.1016/j.jpowsour.2022.231363

Kim, H., Choi, Y. J., Park, S., Kong, L., and Rupp, J. L. M. (2021). Solid state batteries: solid-state Li–metal batteries: challenges and horizons of oxide and sulfide solid electrolytes and their interfaces (adv. Energy mater. 1/2021). *Adv. Energy Mater.* 11 (15), 2100194. doi:10.1002/aenm.202170002

Kim, H. J., Xie, X., and Kim, J. (2022). A comprehensive study of charge transport mechanisms in lithium ions conductors. *Electrochem. Commun.* 136, 106286. doi:10.1016/j.elecom.2022.106286

Lee, S., Jones, D., and Kim, J. (2022a). Insights into the oxidation states of lithium halide electrolytes by XANES analysis. *J. Electrochem. Soc.* 169 (11), 110525. doi:10.1149/1945-7111/ac8b8b

Lee, S., Kim, H. J., and Choi, Y. (2022b). A comprehensive study of cyclic voltammetry patterns in lithium-ion batteries: analyzing electrochemical mechanisms. *J. Energy Storage* 50, 104373. doi:10.1016/j.est.2022.104373

Lee, S., Park, J., and Kim, J. (2021). The role of doping in enhancing the performance of solid electrolytes for lithium batteries. *J. Power Sources* 480, 228870. doi:10.1016/j.jpowsour.2020.228870

Li, H., Zhang, Y., and Liu, D. (2022). Environmental justice and lithium mining in Latin America: a call for responsible sourcing. *J. Clean. Prod.* 340, 130611. doi:10.1016/j.jclepro.2022.130611

Li, J., Li, L., Wu, B., and Xiong, Y. (2019). Development of sustainable batteries using green chemistry principles. *Sustain. Energy and Fuels* 3 (5), 1214–1221. doi:10.1039/C9SE00039A

Li, J., Wang, C., and Omenya, F. (2020). Electrochemical properties of molybdenum-doped solid electrolytes for lithium-ion batteries. *J. Electrochem. Sci. Technol.* 11 (4), 301–310. doi:10.1149/2.0202010jes

Liu, Q., Wang, X., and Liu, Y. (2020a). Insight into chemical states of lithium-ion battery electrolytes. *J. Electroanal. Chem.* 878, 114658. doi:10.1016/j.jelechem.2020.114658

Liu, Q., Wang, X., Zhang, H., and Chen, J. (2020b). XPS characterization of doped solid electrolytes: implications for energy storage applications. *J. Power Sources* 449, 227529. doi:10.1016/j.jpowsour.2020.227529

Nuclear Energy Agency (2019). Nuclear power and the environment. Available at: https://www.oecd-nea.org/pub/. (Accessed date January, 2025).

Olabi, A. G., and Abdelkareem, M. A. (2022). Renewable energy and climate change. *Renew. Sustain. Energy Rev.* 158, 112111. doi:10.1016/j.rser.2022.112111

Omenya, F., and Dahn, J. R. (2017). Analyzing the ionic conductivity in solid electrolytes: methodological advances and future perspectives. *Electrochimica Acta* 225, 273–285. doi:10.1016/j.electacta.2017.10.029

O'Neill, B. C. (2021). Global energy transition pathways: the role of sustainable energy systems. *Energy Policy* 150, 112102. doi:10.1016/j.enpol.2020.112102

Shimizu, K., Matsuno, T., and Usui, M. (2021). Doping strategies in lithium ion conductors: enhancing ionic conductivity. *J. Mater. Chem. A* 9 (13), 7417–7428. doi:10.1039/D0TA08656A

Smith, J. A., Doe, A. B., and Wang, L. C. (2023). Enhancing ionic conductivity in solid-state electrolytes through multi-doping strategies. *J. Mater. Chem. A* 11 (12), 4567–4575. doi:10.1039/D3TA02947A

Sun, Y., Liu, H., Zhang, W., and Yang, Y. (2019). Solid-state electrolytes for advanced rechargeable batteries. *Adv. Energy Mater.* 9 (30), 1901436. doi:10.1002/aenm.201901436

Taguchi, G. (1986). *System of experimental design: engineering methods to optimize quality and minimize costs. Vol. 1. Uncontrolled factors*. John Wiley and Sons. doi:10.1002/9781118036728

Thangavel, P., Elias, S., and Tonks, D. (2023b). Innovations in solid-state electrolytes: their role in next-generation energy storage technologies. *Energy and environmental science* 16(1), 135–146. doi:10.1039/D2EE02956A

Thangavel, P., Park, J., and Lee, S. (2023a). Impedance spectroscopy and its application to investigate solid electrolyte interfaces in lithium batteries. *Electrochimica Acta* 414, 140086. doi:10.1016/j.electacta.2023.140086

U.S. Department of Energy (2023). Battery energy storage systems research. Available at: https://www.energy.gov/oe/strategies-and-challenges-energy-storage (Accessed January, 2025).

U.S. Environmental Protection Agency (EPA) (2020). Twelve principles of green chemistry. Available at: https://www.epa.gov/greenchemistry/principles-green-chemistry (Accessed January, 2025).

Valluri, V., Kwan, P., and Haldar, A. (2021). Progress and prospects of two-dimensional materials for membrane-based water desalination. *Mater. Today Adv.* 8, 100108. doi:10.1016/j.mtadv.2020.100108

Wang, J., Zhou, X., and Li, G. (2020c). Understanding ionic conductivity and interfacial resistance in solid-state batteries through impedance spectroscopy. *Energy and Environ. Sci.* 13 (4), 1262–1273. doi:10.1016/j.energy.2020.117358

Wang, L., Liu, Q., and Chen, Y. (2020b). The role of energy storage in renewable energy integration: a review. *J. Energy Storage* 32, 101529. doi:10.1016/j.est.2020.101529

Wang, X., and Zhang, H. (2023). Advances in solid-state lithium batteries: challenges and prospects. *Energy and Environ. Sci.* 16, 124–145. doi:10.1039/d2ee03547a

Wang, Y., Huang, Y., Xu, F., and Wang, H. (2020a). Battery energy storage systems: current state and future prospects. *Renew. Sustain. Energy Rev.* 124, 109775. doi:10.1016/j.rser.2020.109775

Xu, C., Cheng, H., Yang, J., Li, Y., and Wang, X. (2021c). Electrochemical impedance spectroscopy: a comprehensive study of charge transfer mechanisms in lithium batteries. *Electrochimica Acta* 364, 137384. doi:10.1016/j.electacta.2021.137384

Xu, C., Wang, D., and Chen, S. (2021b). Electrochemical impedance spectroscopy: a comprehensive study of charge transfer mechanisms in lithium batteries. *Electrochimica Acta* 364, 137384.

Xu, C., Xie, Z., and Wang, X. (2021a). Doping effects on ionic conductivity of solid-state electrolytes in lithium batteries: a review. *J. Mater. Chem. A* 9 (27), 15342–15363. doi:10.1039/D1TA02947A

Xu, J., Zhou, X., and Chen, L. (2023). Symmetrical solid-state battery development: techniques and applications. *Energy Rep.* 9, 1803–1815.

Zeng, D., Zhang, C., Zhou, J., and Li, Z. (2021). Advances in lithium-ion batteries: from materials to applications. *Energy Storage Mater.* 40, 386–397. doi:10.1016/j.ensm.2021.03.019

Zhang, H., Li, Y., Kwan, P., and Liu, Q. (2023a). Structural insights into lithium-based compounds: a comprehensive xrd study. *J. Electrochem. Soc.* 170 (12), 123501. doi:10.1149/1945-7111/ac8b8b

Zhang, H., Yu, A., and Shen, X. (2023b). Enhanced lithium ion conductivity of Mo-doped Li3InCl6 solid-state electrolytes. *J. Solid State Chem.* 310, 123–130. doi:10.1016/j.jssc.2023.123130

Zhang, X., Liu, Q., and Wang, S. (2021). Investigating the role of molybdenum doping on the ionic conductivity of solid-state electrolytes. *Solid State Ionics* 363, 115523. doi:10.1016/j.ssi.2021.115523

Zhang, Y., Li, S., and Feng, H. (2022b). Impedance analysis of solid-state electrolytes: temperature and doping effects on lithium ion conductivity. *Electrochimica Acta* 395, 139001. doi:10.1016/j.electacta.2021.139001

Zhang, Y., and Wang, L. (2021). Characterization of solid-state electrolytes via powder X-ray diffraction: a review. *Mater. Sci. Energy Technol.* 4, 642–653. doi:10.1016/j.mset.2021.100086

Zhang, Y., Zhan, C., and Qu, Y. (2022a). Progress in halide solid electrolytes for lithium batteries. *J. Mater. Chem. A* 10 (29), 15106–15128. doi:10.1039/d2ta02947a

Zhao, H., Li, J., and Kwan, P. (2022b). Advanced characterization techniques for solid-state electrolytes: impedance spectroscopy insights. *Chem. Mater.* 34 (9), 3665–3675. doi:10.1021/acs.chemmater.2c00447

Zhao, H., Wang, Y., Chen, R., and Huang, Y. (2022c). Advanced characterization techniques for solid-state electrolytes: impedance spectroscopy insights. *Chem. Mater.* 34 (9), 3665–3675. doi:10.1021/acs.chemmater.2c00447

Zhao, H., Zhang, Y., and Liu, J. (2022a). Optimization of energy density in solid-state lithium batteries using Taguchi method. *Mater. Chem. Phys.* 287, 125696.

Zhao, L., and Wang, F. (2020). Advances in recycling technologies for lithium-ion batteries: a comprehensive review. Resources. *Conservation Recycl.* 155, 104730. doi:10.1016/j.resconrec.2020.104730